Metal π Complexes of Benzene Derivatives. Germanium in the Periphery of Bis(benzene)vanadium and Bis(benzene)chromium. Synthesis and Structure of New Heterametallocyclophanes[†,1]

Christoph Elschenbroich,* Eckhardt Schmidt, Rolf Gondrum, Bernhard Metz, Olaf Burghaus, Werner Massa, and S. Wocadlo

Fachbereich Chemie der Philipps-Universität, D-35032 Marburg, Germany

Received March 24, 1997[⊗]

Mono- and digerma[*n*]metallocyclophanes (n = 1, 2) [($\eta^6,\eta^{6'}$-dimethyldiphenylgermane)M] (M = Cr, **17**; V, **18**•), [($\eta^6,\eta^{6'}$-tetraphenylgermane)M] (M = Cr, **20**; V, **21**•), and [(1,1,2,2-tetramethyl-1,2-di-$\eta^6,\eta^{6'}$-phenyldigermane)Cr] (**24**) were synthesized by means of lithiation and subsequent reaction with dichlorodimethylgermane or dichlorodiphenylgermane. Metal−ligand cocondensation of bromodimethylphenylgermane with chromium atoms followed by reductive coupling with lithium naphthalide gave the digermane complex **24**. Additionally, the nonbridged derivatives [bis(trimethylgermyl-η^6-benzene)M] (M = Cr, **10d**; V, **11**•), [(trimethylgermyl-η^6-benzene)(η^6-benzene)Cr] (**10m**), and [bis(triphenylgermyl-η^6-benzene)M] (M = Cr, **14**; V, **15**•) were prepared and characterized by ^{1}H- and ^{13}C-NMR (**10m**, **10d**, **14**, **17**, **20**), cyclic voltammetry (CV) (**10d**, **11**•, **14**, **15**•, **18**•, **21**•, **24**), and EPR spectroscopy (**10d**•$^+$, **11**•, **14**•$^+$, **15**•, **18**•, **21**•, **24**•$^+$). Crystals of **20** were subjected to a structure determination by X-ray diffraction, which disclosed a bending of the sandwich axis from linearity by 14.4°. The strain exerted on the coordinated benzene ring forces a pyramidal structure on the ipso-C leading to a markedly shielded ^{13}C-NMR resonance. An EPR spectroscopic investigation of the vanadium derivatives reveals an increasing metal to ligand spin delocalization and the appearance of orthorhombic **g** and **A** tensors on bending the sandwich axis. While the redox potentials are virtually unaffected, when passing from the unstrained vanadium complexes **11**• and **15**• to the germa[1]vanadocyclophanes **18**• and **21**•, the transient monocationic species of the latter are destabilized dramatically. No evidence of ring-opening polymerization was observed on heating **18**• to 165 °C. Instead, metal−ligand cleavage occurs.

Introduction

Attachment of short interannular bridges to bis(η^6-arene)metal units leads to heterametallocyclophanes, a class of molecules which lends itself to the study of the influence exerted by distortion of the sandwich unit on chemical and spectroscopic properties. Whereas examples featuring one-atom carbon bridges have not as yet been forthcoming, the larger covalent radii of Si and Zr allowed the synthesis of the hetera[1]metallocyclophanes **1**•,[2] **2**•,[3] **3**,[3,4] **4**,[3] **5**•,[5] and **6**.[5]

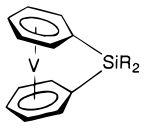

1 R = Me
2 R = Ph

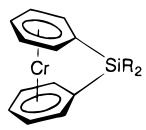

3 R = Me
4 R = Ph

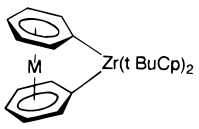

5 M = V
6 M = Cr

Conspicuous features of these strained sandwich complexes include the ease of protodesilylation and, compared to the unsubstituted parent molecules, the anodic shifts of the redox potentials as well as the increase in metal → ligand spin delocalization effected by bending of the bis(arene)metal unit.[3] We have prepared a variety of derivatives of bis(benzene)chromium (**7**) and bis(benzene)vanadium (**8**•) which bear substituents bonded to the η^6-arene via a group 14 element (C, Si, Ge, Sn, Pb).[6] Here we report on new organogermyl arene complexes of V and Cr and compare their properties with those of the silicon analogues. Since the redox potentials $E_{1/2}$ and hyperfine coupling constants a(^{51}V) are highly sensitive to changes in the ligand periphery, even small differences in the covalent radii (Si 1.17, Ge 1.22 Å) and the attendant changes in C−E bond lengths and angles of tilt may trigger measurable responses. Furthermore, the decrease in bond strength (C−Si 301, C−Ge 237 kJ mol^{-1}) may have the effect that rupture of the interannular link occurs at lower temperatures for >GeR_2, compared to >SiR_2 bridges. This could possibly lead to thermal ring-

[†] Dedicated to Professor Gottfried Huttner on the occasion of his 60th birthday.

[⊗] Abstract published in *Advance ACS Abstracts*, September 1, 1997.

(1) Metal π Complexes of Benzene Derivatives. 51. Part 50: Elschenbroich, Ch.; Kühlkamp, P.; Koch, J.; Behrendt, A. *Chem. Ber.* **1996**, *129*, 871.

(2) Hurley, J. Ph.D. Thesis, Philipps-Universität, Marburg, Germany, 1989.

(3) Elschenbroich, Ch.; Hurley, J.; Metz, B.; Massa, W.; Baum, G. *Organometallics* **1990**, *9*, 889.

(4) Hultzsch, K. C.; Nelson, J. M.; Lough, A. J.; Manners, I. *Organometallics* **1995**, *14*, 5496.

(5) Elschenbroich, Ch.; Schmidt, E.; Metz, B.; Harms, K. *Organometallics* **1995**, *14*, 4043.

(6) Schmidt, E. Diplomarbeit, Philipps-Universität, Marburg, Germany, 1988; Doktorarbeit, Philipps-Universität, Marburg, Germany, 1991.

S0276-7333(97)00249-5 CCC: $14.00

Scheme 1

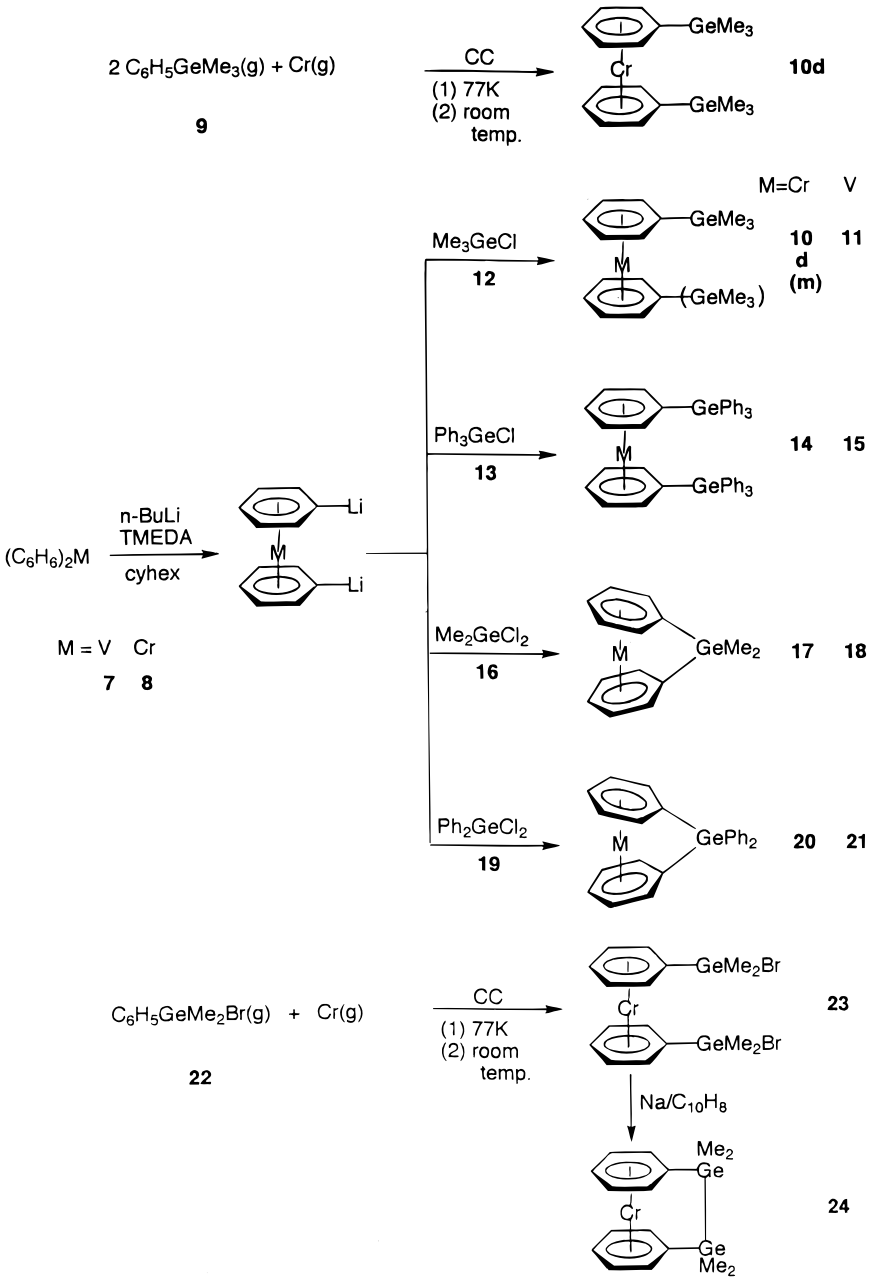

opening polymerization for the $>GeR_2$ derivatives,[7] a process which failed for the $>SiR_2$ analogues **3** and **4**.[4]

Results and Discussion

The new organogermyl derivatives **10**, **11•**, **14**, **15•**, **17**, **18•**, **20**, **21•**, **23**, and **24** were prepared as shown in Scheme 1. They are air- and moisture-sensitive, the maximum of sensitivity being displayed by compounds **17** and **18•**. However, in the unstrained species protolytic cleavage of the C(η-arene)−Ge bonds occurs less readily than in the corresponding organosilyl derivatives: the organogermyl complexes **10** and **14** can be subjected to the purification cycle: $(complex)^0$ $(+O_2) \rightarrow$ $(complex)^+$ $(+Na_2S_2O_4/NaOH) \rightarrow (complex)^0$. Under these conditions quantitative desilylation would take place.

In order to test whether the new germa[1]metallocyclophanes can be converted into bis(arene)metal backbone polymers, the thermal behavior of **18•** was checked. Whereas the ferrocene analogue $[(\eta^5\text{-}C_5H_4)_2\text{-}GeMe_2]Fe$ was reported to undergo rapid thermal ring-opening polymerization when heated in the melt[7], $[(\eta^6\text{-}C_6H_5)_2GeMe_2]V$ (**18•**) decomposes at 160−165 °C prior to melting. If the thermolysis is carried out in an evacuated tube, a black solid residue and a metallic mirror form at the bottom of the tube; droplets of a pale yellow liquid collect at cooler, upper sections. The condensate contains the free ligand Ph_2GeMe_2, identified by means of mass spectrometry.

Crystals suitable for an X-ray structural analysis were obtained for complex **20**. In view of the importance of the structural data for further discussion, they will be presented first.

Molecular Geometry of $[(C_6H_5)_2Ge(\eta^6\text{-}C_6H_5)_2]Cr$ (20). An ORTEP drawing of the structure of **20** in the

(7) Foucher, D. A.; Edwards, M.; Burrow, R. A.; Lough, A. J.; Manners, I., *Organometallics* **1994**, *13*, 4959.
(8) Elschenbroich, Ch. *J. Organomet. Chem.* **1970**, *22*, 677.

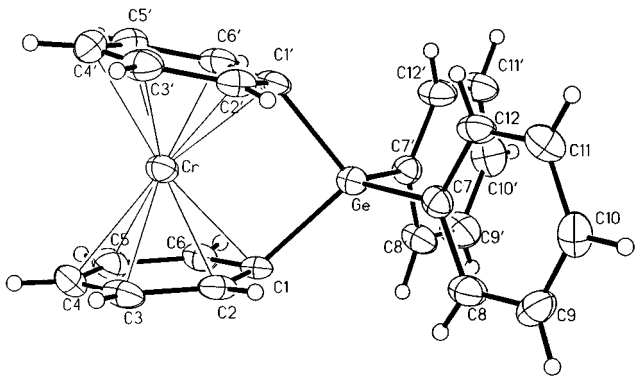

Figure 1. Molecular structure of compound **20** in the crystal. Ellipsoids are drawn at the 50% level.

Table 1. Selected Bond Lengths (Å) and Bond Angles (deg) in [$(C_6H_5)_2Ge(\eta^6\text{-}C_6H_5)_2$]Cr (20)

Cr−C1	2.130(3)	Cr−C2	2.126(3)
Cr−C3	2.160(3)	Cr−C4	2.179(4)
Cr−C5	2.163(4)	Cr−C6	2.127(4)
Cr−C1′	2.122(3)	Cr−C2′	2.126(3)
Cr−C3′	2.159(4)	Cr−C4′	2.167(4)
Cr−C5′	2.156(4)	Cr−C6′	2.127(3)
Ge−C1	1.974(3)	Ge−C7	1.941(3)
Ge−C1′	1.968(3)	Ge−C7′	1.944(3)
C1−C2	1.432(5)	C1−C6	1.418(5)
C2−C3	1.407(5)	C3−C4	1.398(5)
C4−C5	1.406(5)	C5−C6	1.419(5)
C7−C12	1.388(5)	C7−C8	1.401(5)
C8−C9	1.374(5)	C9−C10	1.380(5)
C10−C11	1.375(5)	C11−C12	1.381(5)
C1′−C2′	1.420(5)	C1′−C6′	1.427(5)
C2′−C3′	1.416(5)	C3′−C4′	1.389(5)
C4′−C5′	1.404(5)	C5′−C6′	1.410(5)
C7′−C12′	1.393(5)	C7′−C8′	1.376(5)
C8′−C9′	1.385(5)	C9′−C10′	1.371(5)
C10′−C11′	1.370(5)	C11′−C12′	1.376(5)
C1−Ge−C1′	91.79(14)	C1−Ge−C7	112.75(14)
C1−Ge−C7′	113.3(2)	C1′−Ge−C7	111.3(2)
C1′−Ge−C7′	114.86(14)	C7−Ge−C7′	111.48(14)
Ge−C1−C2	113.7(2)	Ge−C1′−C2′	114.6(2)
Ge−C1−C6	115.1(2)	Ge−C1′−C6′	115.1(2)
C2−C1−C6	116.8(3)	C2′−C1′−C6′	116.7(3)
C1−C2−C3	121.2(3)	C1′−C2′−C3′	121.5(3)
C2−C3−C4	120.9(3)	C2′−C3′−C4′	120.4(3)
C3−C4−C5	119.2(3)	C3′−C4′−C5′	119.7(4)
C4−C5−C6	120.2(3)	C4′−C5′−C6′	120.2(3)
C1−C6−C5	121.5(3)	C1′−C6′−C5′	121.4(3)
Ge−C7−C8	121.0(3)	Ge−C7′−C8′	121.8(3)
Ge−C7−C12	121.3(3)	Ge−G7′−C12′	120.5(3)
C8−C7−C12	117.7(3)	C8′−C7′−C12′	117.6(3)
C7−C8−C9	120.9(3)	C7′−C8′−C9′	121.1(3)
C8−C9−C10	120.2(3)	C8′−C9′−C10′	120.0(4)
C10−C11−C12	119.9(3)	C10′−C11′−C12′	119.6(4)
C7−C12−C11	121.3(3)	C7′−C12′−C11′	121.6(3)

crystal is shown in Figure 1, and bond lengths and bond angles are collected in Table 1. As expected, the structure of **20** mimics that of the silicon analogue **4**. Yet, it is interesting to explore to what extent the increase in covalent radius from Si to Ge translates into structural parameters of the complexes. Slippage is virtually absent in **20** since the perpendicular projection of the chromium atom on the ring least-squares planes deviates from the ring centers by less than 0.05 Å. Surprisingly, the tilting of the η^6-arene ligands is unaffected by exchanging Si for Ge in the interannular bridge in that, for both complexes **4**[3] and **20**, the sandwich axis is bent by 14.4(2)°. This contrasts with the increase in tilting angle from 14.4(2)° to 19.9(1)° [9] upon change of the central metal atom from chromium to vanadium, retaining the heteroatom Si in the bridge. This is a consequence of the larger inter-arene distance in bis(benzene)vanadium (3.32 Å[10]) compared to that in bis(benzene)chromium (3.22 Å[11]). Marked differences are, however, observed in the geometry of the bridges $>EPh_2$ (E = Si, Ge): the angle C1−E−C1′ is more acute for E = Ge (91.8(2)°) than for E = Si (96.0(2)° [3]). A similar gradation has been observed for the couple $[Me_2E(\eta^6\text{-}C_5H_4)_2]Fe$, E = Si, Ge.[7]

In concordance with equal tilting angles for **20** and **4**, the angle between the E−C1 (or F−C1′) bond axis and the respective η^6-arene decreases by 2.1° upon the change from E = Si (40.8(2)°) to E = Ge (38.7(2)°). The distance Cr···E between the central metal atom and the group 14 element in the interannular bridge slightly increases from 2.842(2) Å (E = Si, **4**[3]) to 2.958(1) Å (E = Ge, **20**).

Nuclear Magnetic Resonance. The NMR data for the new organogermylarene complexes reported here closely resemble those for the organosilyl analogues[3] and therefore do not need extensive discussion. Attention should, however, be drawn to the most characteristic feature, which consists in the extremely large coordination shift $\Delta\delta(^{13}C)$ experienced by the ipso-C resonance in the germa[1]chromocyclophane **20**. As depicted in Scheme 2, the upfield shift caused by the bending distortion at the carbon atoms which are involved in the interannular bridge is comparable in magnitude to the shift brought about by metal coordination. This phenomenon has been traced to a change in carbon hybridization from sp^2 toward sp^3.[3,7,12]

Electron Paramagnetic Resonance. The influence tilting exerts on the EPR properties of bis(arene)-metal radicals has concerned us before[3,13] because an analysis of the **g** tensor may help to describe the structure of paramagnetic sandwich complexes in cases where NMR and X-ray diffraction data are unavailable. Furthermore, it furnishes information on the extent of metal−ligand spin delocalization thereby providing hints at the electronic structure. EPR spectra of the vanadium complexes are depicted in Figure 2 (**11**$^{\bullet}$, **18**$^{\bullet}$), and the EPR parameters for these neutral species, together with those for the chromium-containing radical cations **10d**$^{\bullet+}$, **14**$^{\bullet+}$, and **24**$^{\bullet+}$, are collected in Table 2. The interannularly bridged radical cations **17**$^{\bullet+}$ and **20**$^{\bullet+}$ are inaccessible (*vide infra*). Inspection of the data reveals that, as in the case of peripheral substitution by R_3Si groups,[3] for the unstrained species **10d**$^{\bullet+}$, **14**$^{\bullet+}$,

(9) Elschenbroich, Ch.; Bretschneider-Hurley, A.; Hurley, J.; Behrendt, A.; Massa, W.; Wocadlo, S.; Reijerse, E. *Inorg. Chem.* **1995**, *34*, 743.

(10) Fischer, E. O.; Fritz, H. P.; Manchot, J.; Priebe, E.; Schneider, R. *Chem. Ber.* **1963**, *96*, 1418.

(11) Haaland, A. *Acta Chem. Scand.* **1965**, *19*, 41. Keulen, E.; Jellinek, F. *J. Organomet. Chem.* **1966**, *5*, 490.

(12) Osborne, A. G.; Whiteley, R. H.; Meads, R. A. *J. Organomet. Chem.* **1980**, *193*, 345.

(13) Elschenbroich, Ch.; Schneider, J.; Prinzbach, H.; Fessner, W. D. *Organometallics* **1986**, *5*, 2091.

(14) The presence of an interannular bridge in **24**$^{+}$ cannot be inferred with confidence from **g** and hyperfine data since they do not differ sufficiently. It is, however, proven by the different extents to which the lines in the high-field ^{53}Cr satellite spectra are broadened, relative to those at low field. Since this $m_I(^{53}Cr)$ dependent broadening correlates with the rate of tumbling in solution and thereby the effective molecular volume, the fact that the low-field/high-field ratio of spectral amplitudes equals 2.26 for **24**$^{\bullet+}$ and 2.61 for the "open" complex **10**$^{\bullet+}$ attests to the presence of an interannular link in **24**$^{\bullet+}$.

(15) Elschenbroich, Ch.; Bilger, E.; Metz, B. *Organometallics* **1991**, *10*, 2823.

(16) Lepeska, B.; Chvalovsky, V. *Collect. Czech. Chem. Commun.* **1970**, *35*, 261.

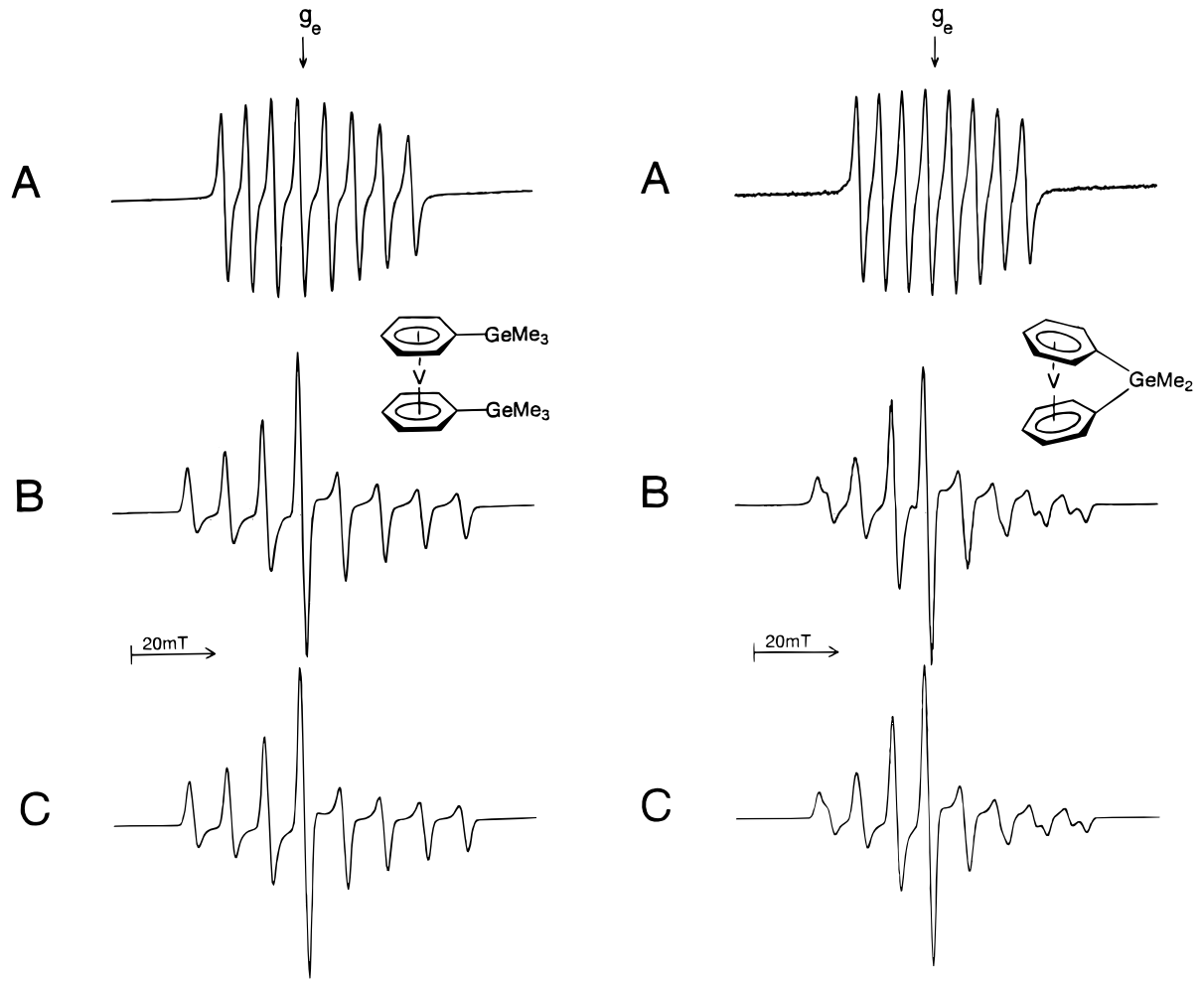

Figure 2. EPR spectra of the methylgermyl derivatives **11**• and **18**• in toluene. A: Fluid solution, 295 K. B: Rigid solution, 140 K. C: Simulation.

Scheme 2

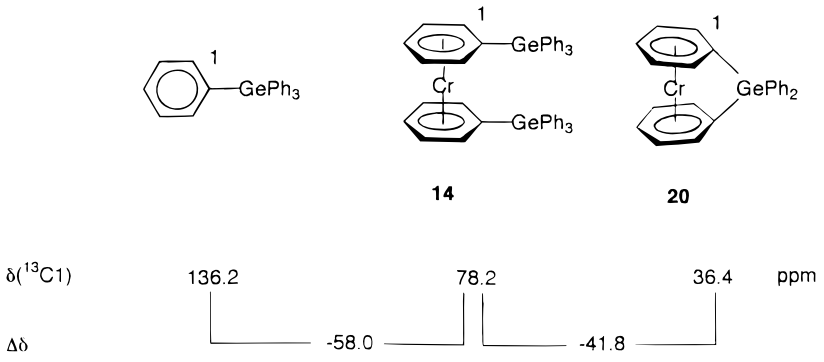

11•, and **15**• an *electronic* effect of R_3Ge groups on the EPR spectra is hardly noticeable. However, the introduction of an interannular bridge $>GeR_2$ results in a change of the **g** and **A**(^{51}V) tensors from effectively axial to rhombic. The differences between the parameters for the perpendicular orientation (indexes 1 and 2 in Table 2) are larger for Ge, as compared to Si as a member of the interannular link. In fact, in the case of **2**• these differences were too small to be resolved. Since the tilt of the sandwich units is virtually unaffected by a substitution of Si by Ge and the distance between the central atom and the heteroatom in the bridge actually increases (compare the structural data for **4** and **20**), one is forced to conclude that it is the *nature* of the bridging atom which governs the magnitude of the perturbation, reflected in the rhombicity of **g** and **A** (^{51}V). While the distances M···E (M = Cr, V; E = Si, Ge) in the tilted complexes under investigation certainly exceed those appropriate for regular covalent bonds, a value of 2.45 Å being derived from atomic radii, weak dative interactions may still be operative. Interactions of this kind have been postulated for the related series of [1]germaferrocenophanes based on Mössbauer spectroscopic results.[7] In the case of the radicals **18**• and **21**• the differentiation between the two equatorial components may be traced to a small contribution by the heteroatom E which raises the degeneracy in the *x*, *y* plane. This effect should be more pronounced for E = Ge than for E = Si, bearing in mind that the spin−orbit coupling constant λ(Ge) exceeds the value λ(Si) by

Table 2. EPR Data for the Complexes 2•, 7•+, 8•, 10d•+, 11•, 14•+, 15•, 18•, 21•, 24•+, and 25•

	8• [a,c]	**11•** [a,f]	**18•** [a,f]	**15•** [a,f]	**21•** [a,f]	**25•**	**2•**	**7•+** [b,c]	**10d•+** [b]	**24•+** [b]	**14•+** [b]
g_{iso}	1.9860[c]	1.9853	1.9872	1.9858	1.9859	1.9864	1.9866	1.9867	1.9861	1.9881	1.9866
g_1			1.9780		1.9765						
$g_2[g_\perp]$	1.978	1.9739	1.9821	1.9754	1.9806	1.980	1.979	1.979			1.9799
$g_3[g_\parallel]$	2.001	1.9988	2.0014	1.9979	2.0000	1.999	2.002	2.002			2.0000
$\langle g \rangle$ (calcd)		1.9835	1.9872	1.9829	1.9857						
$a(^{53}Cr,^{51}V)$[d]	6.38	6.330	5.611	6.461	5.636	6.34	5.63	1.81	1.80	1.77	1.80
$a(^{1}H)$[d]	0.40					0.40		0.338	0.331	0.301	0.302
$A_1(^{53}Cr,^{51}V)$[d]			9.032		8.979						
$A_2(^{53}Cr,^{51}V)[A_\perp]$[d]	9.25	9.245	7.998	9.171	8.063	9.31	8.50	2.69			
$A_3(^{53}Cr,^{51}V)[A_\parallel]$[d]	0.64	0.489	−0.149	1.037	−0.128	0.40	0	0.05			
$\langle A(^{53}Cr,^{51}V)\rangle$[d]		6.330	5.627	6.460	5.638						

[a] In toluene. [b] In 1:1 $CHCl_3$/DMF. [c] Reference 3. [d] In mT. [f] Data obtained through fit routine program CWSIM, ref 18. [g] Anisotropy incompletely resolved.

a factor of 5.[17] Axial **g** and **A**(^{51}V)-hyperfine tensors wereobserved, however, for the complex **5•**, which contains zirconium in the one-atom interannular link.[5] This zircona[1]vanadocyclophane is only minimally distorted from axiality (tilt angle 3.7°), and the considerably larger distance V···Zr of 3.25(2) Å (sum of covalent radii = 2.76 Å) should preclude the type of dative interaction which was postulated for the germanium-linked complexes **18•** and **21•** to account for the EPR features. As has been demonstrated before,[5] tilting of the bis(η^6-arene)vanadium unit also modifies the isotropic hyperfine coupling constant $a(^{51}V)$; in concordance with the similar tilt angle for the complexes **2•** and **21•**, a considerably decreased value $a(^{51}V)$ = 5.63 mT is observed for both [1]vanadocyclophanes whereas the nonbridged, untilted complexes possess $a(^{51}V)$ parameters of 6.34 ($(Ph_3Si\text{-}\eta^6\text{-}C_6H_5)_2V$) (**25•**), 6.33 (**11•**), and 6.46 mT (**15•**), respectively. This effect has been interpreted in terms of more extensive metal−ligand orbital mixing which accompanies the deviation from axial symmetry. A less than 2% decrease in the coupling constant $a(^{53}Cr)$ is observed upon proceeding from $[(Me_3Ge\text{-}\eta^6\text{-}C_6H_5)_2Cr]^{\bullet+}$ (**10•+**) to the 1,2-digerma[2]chromocyclophane **24•+**. Due to the larger bridge, $Me_2GeGeMe_2$, **24** is unstrained and the two η^6-arenes should maintain their parallel disposition. Therefore, as in the case of the zircona[1]vanadocyclophane **5•** [5] (tilting angle 3.7°) spin distribution is not markedly changed. Presumably it is the lack of strain to which the radical cation **24•+** owes its existence.[14]

Cyclic Voltammetry. The redox behavior of the organogermanyl derivatives of bis(benzene)vanadium and bis(benzene)chromium is represented by cyclic voltammetric traces (Figure 3) and by the pertaining parameters, which are collected in Table 3. Reversible or at least partly reversible reductions are only observed for the vanadium species where electron transfer leads to an 18 valence electron configuration at the central metal atom. Anions which are stable on the time scale of the CV experiment are also obtained for the derivatives **18•** and **21•**, which contain the one-atom interannular bridges $>GeMe_2$ and $>GePh_2$, respectively. For the vanadium complexes, electrochemical oxidation is reversible if the two rings carry individual R_3Ge groups

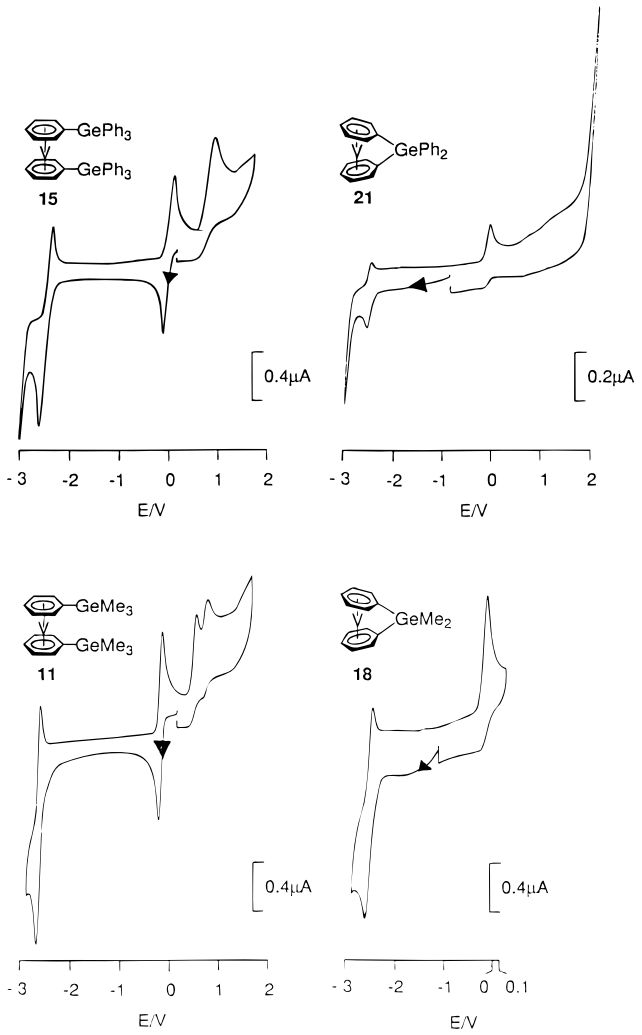

Figure 3. Cyclic voltammetric traces for the complexes **15•**, **18•**, **11•**, and **21•** at −50 °C in 1,2-dimethoxyethane/0.1 M tetrabutylammonium perchlorate: working electrode, glassy carbon; reference electrode, SCE.

but irreversible if a one-membered interannular link $>R_2Ge$ is present.

The solvolytic cleavage of the one-membered interannular bridge in the corresponding chromium complexes prevents a study of their electrochemical behavior. However, a two-membered interannular link, $GeMe_2GeMe_2$, confers reversibility on the oxidation of **24**. It may therefore be concluded, that the cleavage of the C_{arene}−Ge bond is initiated by electrophilic attack at the ipso carbon atom which in the case of the strained tilted germa[1]metallocyclophanes **17** and **20** carries high electron density, as implied by the NMR data.

(17) (a) Lu, C. C.; Carlson, T. A.; Malik, F. B.; Tucker, T. C.; Nestor, C. W., Jr. *Atomic Data* **1971**, *3*, 1. Carlson, T. A. *Photoelectron and Auger Spectroscopy*; Plenum Press: New York, 1975; p 113 f. (b) Klapötke, T. M.; Schulz, A. *Quantenmechanische Methoden in der Hauptgruppenchemie*; Spektrum Akademischer Verlag: Heidelberg, 1996; p 177.

(18) Burghaus, O. University of Marburg, unpublished data.

Table 3. Cyclic Voltammetric Data for the Compounds 10d, 11•, 14, 15•, 18•, 21•, 24, 8•, and the Standard 7•

	$E_{1/2}(0/-)$/V[b]	ΔE_p/mV[b]	r[b]	$E_{1/2}(+/0)$/V[b]	ΔE_p/mV[b]	r[b]	E_{pa}[e]/V	E_{pa}[e]/V
10d[c]	−2.64[e]			−0.65	76	1.0	0.99	
11[d,g]	−2.66	75	∼0.5	−0.30	61	1.0	0.35	0.57
14[c]				−0.54	62	1.0	1.08	
15[d]	−2.52	110	∼0.6	−0.17	73	1.0	0.66	
18[d]	−2.62	78	∼0.6	−0.31[e]				
21[d]	−2.59	74	∼0.8	−0.19[e]				
24[c]				−0.69	91	1.0	1.07	
8[f]	−2.71	74	0.93	−0.35	66	1.0	0.24	0.46
7[d,g]	<−3.1			−0.73	65			

[a] In 1,2-dimethoxyethane/0.1 M tetraethylammonium perchlorate at a glassy carbon electrode *versus* a saturated calomel electrode. [b] $E_{1/2} = {}^1/_2(E_{pa} + E_{pc})$, $\Delta E_p = E_{pa} - E_{pc}$, $r = I_{p(fwd)}/I_{p(rev)}$. [c] At 20 °C. [d] At −50 °C. [e] Peak potential of an irreversible wave. [f] At −35 °C, ref 15. [g] Determined in a sample solution which was 4.65×10^{-3} M both in **11•** and in **7**. Identical peak heights for **11** and the reversible standard **7** attest to the 1e nature of the redox processes. The current function $I_p/\nu^{1/2}$ proved to be independent of scan rate ($50 < \nu < 400$ mV s^{-1}).

We reported earlier that the substitution of a hydrogen atom by a $SiPh_3$ group causes an anodic shift of about 95 mV per $SiPh_3$ group for the reduction potential $E_{1/2}(0/-)$ of the bis(η^6-arene)vanadium unit.[3] The slightly smaller value found for the $GePh_3$ substituent (75 mV per $GePh_3$ group) reflects the small differences in electronegativity between silicon and germanium. (Allred-Rochow values: C 2.50, Si 1.74, Ge 2.02). The reduction of **11•**, the trimethylgermyl analogue of **15•**, is not fully reversible. This is probably due to interference of the reduction of the coordinated ligand **9**, which gives rise to an irreversible wave in the chromium complex [(Me_3Ge-η^6-C_6H_5)$_2$Cr] **(10d)** at −2.64 V. Thus, in order to evaluate the electronic effect of the $GeMe_3$ group, it is necessary to compare the reversible oxidations of $\mathbf{15}^{+/0}$ and $\mathbf{11}^{+/0}$ with that of $\mathbf{8}^{+/0}$. The differences $E_{1/2}(\mathbf{15}^{+/0}) - E_{1/2}(\mathbf{8}^{+/0}) = 190$ mV and $E_{1/2}(\mathbf{11}^{+/0}) - E_{1/2}(\mathbf{8}^{+/0}) = 50$ mV indicate that the anodic shift decreases on exchanging phenyl by methyl groups. This gradation is expected in view of the larger acceptor capability of phenyl vs methyl.

Assessing the effect exerted by bending of the sandwich axis on the redox potentials is hampered by the unknown electronic influences the interannular bridge inflicts on the energy of the redox orbital. As a rough guess one may assume that the effect of substitution of one hydrogen atom for a $GePh_3$ group (75 mV) is comparable to the exchange of two hydrogens by an interannular $GePh_2$ link. Under this assumption the difference of the reduction potentials of [Ph_2Ge(η^6-C_6H_5)$_2$]V (**21•**) and the parent complex **8•** (80 mV) should be a superposition of substitutional (75 mV) and bending (5 mV) effects. For the silicon analogue [Ph_2Si(η^6-C_6H_5)$_2$]V (**2•**) a small bending influence of 35 mV was calculated using the same approach.[3] Taking into account that [Ph_2Ge(η^6-C_6H_5)$_2$]Cr (**20**) and [Ph_2Si(η^6-C_6H_5)$_2$Cr] (**4**) have identical ring tilts, it may be concluded that the effect exerted on the redox behavior by bending of the sandwich structure is, at best, marginal. This lack of response is not unexpected if it is borne in mind that the redox orbital is metal centered and nonbonding. Therefore, variations in the ligand periphery should influence the redox orbital only indirectly by effecting a small change in the partial charge on the central metal atom. By way of contrast, the 14.4(2)° sandwich tilt is clearly reflected in the nonaxiality of the **g** tensor for **18•** and **21•** (Table 2). This, again, is in concordance with expectation since the deviations of g_x and g_y from 2.0023 result from mixing of the singly occupied orbital $a_1(V(3d_{z^2}))$ with molecular orbitals whose degeneracies have been raised by the structural distortion.

Experimental Section

Chemical manipulations and physical measurements were carried out using techniques and instruments specified previously.[3]

Crystal Structure Determination of [(C_6H_5)$_2$Ge(η^6-C_6H_5)$_2$]Cr (20). A crystal of **20** was grown from a saturated solution in toluene at 4 °C. Data were collected on a four circle diffractometer (CAD4, Enraf-Nonius) at room temperature. The structure was solved in the monoclinic space group $P2_1/n$ ($a = 7.695(2)$ Å, $b = 18.794(4)$ Å, $c = 12.729(3)$ Å, $\beta = 94.34(3)$°) using Patterson methods and difference Fourier syntheses. All atoms including the hydrogen atoms were localized. The refinement, however, was performed with hydrogen atoms in calculated positions (d(C−H) = 0.96 Å) with common isotropic temperature factors. The final residuals were wR_2 = 0.072 for all 2223 independent reflections corresponding to $R_1 = 0.028$ for the observed reflections ($F_0 > 4\sigma(F_0)$). Bond lengths, angles, and the data collection and refinement parameters are listed in Tables 1 and 4, respectively. Atomic coordinates and displacement parameters have been deposited with the Fachinformationszentrum Karlsruhe, Gesellschaft für wissenschaftlich-technische Information mbH, D-76344 Eggenstein-Leopoldshafen, Germany; Depository No. CSD 405 982.

[Me_3Ge-η^6-C_6H_5]$_2$Cr (10d). Cocondensation route: In a 2 L reactor, chromium (0.5 g, 9.6 mmol) is evaporated from a resistively heated tungsten spiral and cocondensed at 77 K during 1.5 h with Me_3GePh (13 g, 70 mmol). After warming to room temperature the reddish brown product is dissolved in 200 mL of toluene, the solution is filtered through Celite, and the solvent is evaporated in vacuo. Yield of crude material: 990 mg (24%). Sublimation at 80 °C/10^{-4} mbar affords pure **10d** as greenish black microcrystalline material (350 mg, 8% yield). ^{1}H NMR (benzene-d_6): δ 4.24 (br, *o*-H), 4.13−4.18 (br, *m*-, *p*-H), 0.29 (s, CH_3). ^{13}C NMR (benzene-d_6): δ 81.1 (ipso-C), 78.3 (*o*-C, ^1J(C,H) = 170 Hz), 76.2 (*m*-C, 166 Hz), 74.8 (*p*-C, 167 Hz), −0.9 (CH_3, 125 Hz). MS (EI, 70 eV): *m*/*z* (relative intensity) 442 (M^+, 18.3), 248 ($M^+ - PhGeMe_3$, 21.2), 181 ($PhGeMe_2^+$, 100), 151 ($PhGe^+$, 14.8), 52 (Cr^+, 27.8). Anal. Calcd for $C_{18}H_{28}CrGe_2$: C, 48.95; H, 6.39. Found: C 49.19; H, 6.48.

[(Me_3Ge-η^6-C_6H_5)(η^6-C_6H_6)]Cr (10m) and [Me_3Ge-η^6-C_6H_5]$_2$Cr (10d). Lithiation route: To a suspension of bis(benzene)chromium (**7**) (3.03 g, 14.6 mmol) in 200 mL of cyclohexane is added at room temperature a 1.6 M solution of *n*-butyllithium in hexane (22.7 mL, 36.4 mmol of *n*-BuLi) and an equimolar amount of *N*,*N*,*N*′,*N*′-tetramethylethylenediamine (5.6 mL, 36.4 mmol). The mixture is refluxed for 1 h and cooled to 0 °C and a solution of trimethylchlorogermane (**12**) (4.5 mL, 36.4 mmol) in 10 mL of cyclohexane is added

Table 4. Crystal Data, Data Collection, and Refinement Parameters for [$(C_6H_5)_2$Ge-(η^6-$C_6H_5)_2$]Cr (20)

formula	$C_{24}H_{20}CrGe$
fw	432.99
temp	293(2) K
wavelength	0.710 73 Å
cryst syst	monoclinic
space group	$P2_1/n$
unit cell dimens	$a = 7.695(2)$ Å
	$b = 18.794(4)$ Å
	$c = 12.729(3)$ Å
	$\alpha = 90°$
	$\beta = 94.34(3)°$
	$\gamma = 90°$
vol	1835.6(8) Å^3
Z	4
D(calcd)	1.567 g cm^{-3}
abs coeff	2.233 mm^{-1}, ψ-scan correction
F(000)	880
cryst size	0.20 × 0.20 × 0.10 mm^3
θ range for data collctn	2.17−21.94°
index range	$-8 \le h \le 8$, $0 \le k \le 19$, $0 \le l \le 13$
no. of reflns collctd	2341
no. of indep reflns	2225 ($R_{int} = 0.0284$)
refinement	full matrix least squares on F^2 (SHELXL-93[a])
data/restraints/params	2223/0/236
goodness-of-fit on F^2	1.087
final R indices [$I > 2\sigma(I)$]	$R_1 = 0.0278$; w$R_2 = 0.0659$
R indices (all data)	$R_1 = 0.0403$; w$R_2 = 0.0718$
largest diff peak and hole	0.485 and −0.371 e Å^{-3}

[a] Sheldrick, G. M. *SHELXL-93, Program for the Refinement of Crystal Structures*; University of Göttingen: Göttingen, Germany, 1993.

during 1 h. The mixture is stirred for another 12 h and filtered and the solvent is removed under reduced pressure. The residue, a dark brown oil, is dissolved in petroleum ether/diethyl ether (3:1) and chromatographed at a silica gel column (20 × 4 cm). The first brown band which is eluted with petroleum ether/diethyl ether contains a mixture of [(Me_3Ge-η^6-C_6H_5)(η^6-C_6H_6)]Cr (**10m**) and [Me_3Ge-η^6-C_6H_5]$_2$Cr (**10d**), which is separated by means of fractional sublimation at a temperature gradient 70 > T > 25 °C. The upper section in the tube contains the brown monosubstituted product **10m** (110 mg, 0.34 mmol, 2.3%) and the lower section the greenish-brown disubstituted product **10d** (820 mg, 1.86 mmol, 12.7%). The second band on the column is eluted with toluene. It contains unreacted bis(benzene)chromium (780 mg, 3.75 mmol, 26%). Higher, yellow bands which can only be eluted with THF have not been analyzed.

Compound **10m**: ^{1}H NMR (THF-d_8) δ 4.31 (*o*-H), 4.24 (*m*-, *p*-H), 4.22 (η-C_6H_6), 0.29 (CH_3); ^{13}C{^{1}H} NMR (THF-d_8) δ 81.5 (ipso-C), 78.6 (*o*-C), 76.1 (*m*-C), 75.0 (*p*-C), 75.1 (C_6H_6), −1.1 (CH_3). Anal. Calcd for $C_{15}H_{20}CrGe$: C, 55.45; H, 6.20. Found: C, 55.56; H, 6.33. Compound **10d**: ^{1}H NMR (THF-d_8) δ 4.33 (*o*-H), 4.25−4.28 (*m*-, *p*-H), 0.33 (CH_3); ^{13}C{^{1}H} NMR (THF-d_8) δ 81.5 (ipso-C), 78.6 (*o*-C), 76.6 (*m*-C), 75.1 (*p*-C), −0.85 (CH_3). Anal. Calcd for $C_{18}H_{28}CrGe_2$: C, 48.95; H, 6.39. Found: C, 48.75; H, 6.49.

[Me_3Ge-η^6-C_6H_5]$_2$V (11•) was prepared via lithiation and subsequent reaction with Me_3GeCl in analogy to the synthesis of **10**. The reaction and subsequent purification procedure afforded brown needles. Yield :56%. EPR: see Table 2. MS (EI, 70 eV): *m*/*z* (relative intensity) 441 (M^+, 19.9), 181 ($PhGeMe_2^+$, 100), 151 ($PhGe^+$, 20.5). Anal. Calcd for $C_{18}H_{28}VGe_2$: C, 49.07; H, 6.42. Found: C, 48.84; H, 6.43.

[Ph_3Ge-η^6-C_6H_5]$_2$Cr (14). To a suspension of bis(benzene)-chromium (**7**) (500 mg, 2.4 mmol) in 100 mL of cyclohexane are added a 1.6 M solution of *n*-butyllithium in hexane (3.6 mL, 5.8 mmol) and *N*,*N*,*N*′,*N*′-tetramethylethylenediamine (0.86 mL, 5.8 mmol). After refluxing for 1.5 h the mixture is cooled to room temperature and decanted to remove monolithiated **7**, which is soluble. The precipitate, which contains 1,1′-dilithiated **7**, is washed with three fractions of petroleum ether (40/60) and suspended in 50 mL of diethyl ether. With vigorous stirring at room temperature is added during 0.5 h 100 mL of a solution of triphenylchlorogermane (**13**) (1.6 g, 4.8 mmol) in diethyl ether. After stirring overnight and filtration, the yellow solid is extracted with 100 mL of boiling toluene. The extract is layered with an equal volume of petroleum ether (40/60) and kept at −25 °C for 24 h. **14** is obtained as a yellow microcrystalline material. Yield: 340 mg (0.42 mmol, 18%). ^{1}H NMR (benzene-d_6): δ 4.40 (*o*-H), 4.23 (*m*-, *p*-H), 7.57 (*o*-H, $GePh_3$), 7.04 (*m*-, *p*-H, $GePh_3$). ^{13}C NMR (benzene-d_6) δ 78.2 (ipso-C), 77.0 (*o*-C), ^1J(C,H) = 167 Hz), 80.4 (*m*-C, 165 Hz), 74.6 (*p*-C, 164 Hz), 137.9 (ipso-C, $GePh_3$), 135.9 (*o*-C, $GePh_3$), 128.6 (*m*-C, $GePh_3$), 129.3 (*p*-C, $GePh_3$). MS (EI, 70 eV): *m*/*z* (relative intensity) 814 (M^+, 19.0), 434 ($M^+ - Ph_3$-Ge, 100), 305 (Ph_3Ge^+, 93.6), 228 (Ph_2Ge^+, 36.6), 151 ($PhGe^+$, 19.5), 52 (Cr^+, 22.7). Anal. Calcd for $C_{48}H_{40}CrGe_2$: C, 70.82; H, 4.95. Found: C, 70.87; H, 3.96.

[Ph_3Ge-η^6-C_6H_5]$_2$V (15•). The synthesis is performed as described for **14**. It affords **15** as a red, microcrystalline material (yield 21%) which decomposes at 295 °C. EPR data: see Table 2. MS (EI, 70 eV): *m*/*z* (relative intensity) 813 (M^+, 37.5), 433 ($M^+ - Ph_3Ge$, 100), 305 (Ph_3Ge^+, 84.6), 228 (Ph_2Ge^+, 57.0), 207 ($C_{12}H_{12}V^+$, 61.0), 151 ($PhGe^+$, 35.4), 51 (V^+, 42.2). Anal. Calcd for $C_{48}H_{40}Ge_2V$: C, 70.91; H, 4.96. Found: C, 71.00; H, 5.01.

[Me_2Ge(η^6-C_6H_5)$_2$]Cr (17). Bis(benzene)chromium (2.5 g, 12 mmol) is lithiated as described above, and the mixture is decanted. The solid is suspended in 150 mL of petroleum ether (40/60), and during 45 min a solution of dimethyldichlorogermane (2.08 g, 12 mmol) in 40 mL of petroleum ether is added at −20 °C. The solution is allowed to warm to room temperature and is stirred for 2 h. Filtration through celite affords a highly air-sensitive reddish-brown solution. Cooling to −25 °C causes precipitation of **17** as greenish brown crystals which decompose at 178−182 °C. Yield: 750 mg (20%). ^{1}H NMR (benzene-d_6): δ 3.81 (*o*-H), 4.66 (*m*-, *p*-H), 0.40 (CH_3). ^{13}C NMR (benzene-d_6): δ 37.5 (ipso-C), 76.5 (*o*-C, ^1J(C,H) = 168 Hz), 83.7 (*m*-C, 165 Hz), 79.1 (*p*-C, 166 Hz), −3.9 (CH_3, 125 Hz). MS (EI, 70 eV): *m*/*z* (relative intensity) 310 (M^+, 79.4), 243 (Ph_2GeMe^+, 90.5), 208 ($C_{12}H_{12}Cr^+$, 49.9), 181 ($PhGeMe_2^+$, 29.1), 151 ($PhGe^+$, 36.9), 130 ($C_6H_6Cr^+$, 67.7), 104 ($GeMe^+$, 10.2), 52 (Cr^+, 100). Anal. Calcd for $C_{14}H_{16}CrGe$: C, 54.44; H, 5.22. Found: C, 53.84; H, 5.01.

[Me_2Ge(η^6-C_6H_5)$_2$]V (18•). The preparation follows the directions given for **17**. Compound **18•** is obtained as brown crystals (yield 34%), which decompose without prior melting at 160−165 °C. EPR data: see Table 2. MS (EI, 70 eV): *m*/*z* (relative intensity) 309 (M^+, 90.5), 279 ($M^+ - 2CH_3$, 55.9), 243 (Ph_2GeMe^+, 100), 207 ($C_{12}H_{12}V^+$, 18.0), 181 ($PhGeMe_2^+$, 38.1), 151 ($PhGe^+$, 81.6), 129 ($C_6H_6V^+$, 17.2), 51 (V^+, 51.3). Anal. Calcd for $C_{14}H_{16}GeV$: C, 54.63; H, 5.24. Found: C, 54.02; H, 5.35.

[Ph_2Ge(η^6-C_6H_5)$_2$]Cr (20). The preparation follows the directions given for **17**, replacing Me_2GeCl_2 by Ph_2GeCl_2 (**19**). The suspension is filtered, the residue is washed with two 50 mL portions of petroleum ether (40/60), and the solid is dissolved in boiling toluene, concentrated *in vacuo*, and cooled to −10 °C. **20** is obtained as small black crystals with a metallic luster (yield 44%). ^{1}H NMR (benzene-d_6): δ 4.22 (*o*-H), 4.66 (*m*-, *p*-H), 7.93−7.96 (*o*-H, $GePh_2$), 7.29−7.32 (*m*-, *p*-H, $GePh_2$). ^{13}C NMR (benzene-d_6): δ 36.4 (ipso-C), 77.8 (*o*-C, ^1J(C,H) = 169 Hz), 83.9 (*m*-C, 165 Hz), 79.5 (*p*-C, 167 Hz), 136.5 (ipso-C, $GePh_2$), 134.6 (*o*-C, $GePh_2$, 159 Hz), 129.3 (*m*-C, $GePh_2$, 159 Hz), 129.9 (*p*-C, $GePh_2$). MS (EI, 70 eV): *m*/*z* (relative intensity) 343 (M^+, 57.3), 305 (Ph_3Ge^+, 100), 228 (Ph_2Ge^+, 82.7), 151 ($PhGe^+$, 39.2), 52 (Cr^+, 63.9). Anal. Calcd for $C_{24}H_{20}CrGe$: C, 66.57; H, 4.66. Found: C, 66.70; H, 4.76.

[Ph_2Ge(η^6-C_6H_5)$_2$]V (21•). The synthesis was as described for **20**. Compound **21•** forms an olive black microcrystalline material which is only sparingly soluble in toluene (yield 29%). EPR data: see Table 2. MS (EI, 70 eV): *m*/*z* (relative

intensity): 433 (M^+, 59.0), 305 (Ph_3Ge^+, 100), 228 (Ph_2Ge^+, 84.9), 151 ($PhGe^+$, 68.8), 51 (V^+, 14.6). Anal. Calcd for $C_{24}H_{20}GeV$: C, 66.73; H, 4.67; Found: C, 66.48; H, 4.52.

(Me_2BrGe-η^6-$C_6H_5)_2Cr$ (23). In a 2 L reactor, cooled with liquid N_2, during a period of 2 h phenyldimethylbromogermane (**22**)[16] (15.0 g, 58 mmol) is cocondensed with chromium vapor (0.5 g, 9.6 mmol). The reddish-brown product is dissolved in toluene at room temperature, the dark red solution is filtered through Celite, and solvent and excessive free ligand are removed *in vacuo*. The residue which appears green (thin layer) or brown (thick layer) may be sublimed under reduced pressure (125 °C, 10^{-4} mbar). Yield: 980 mg (18%). ^{1}H NMR (benzene-d_6): δ 4.16 (br, *o*-, *m*-, *p*-H), 0.71 (CH_3). $^{13}C\{^1H\}$ NMR (benzene-d_6): δ 80.0 (ipso-C), 78.4 (*o*-C), 76.8 (*m*-C), 75.2 (*p*-C), 4.70 (CH_3). MS (EI, 70 eV): *m*/*z* (relative intensity): 572 (M^+, 5.2), 312 (M^+ − L, 52.6), 181 ($PhGeMe_2^+$, 100), 151 ($PhGe^+$, 20.3), 52 (Cr^+, 20.9). Anal. Calcd for $C_{16}H_{22}Br_2CrGe_2$: C, 33.63; H, 3.88. Found: C, 33.88; H, 4.13.

[Me_4Ge_2-1,2-(η^6-$C_6H_5)_2$]Cr (24). From freshly sublimed naphthalene (0.75 g, 58 mmol) and sodium (124 mg, 5.4 mmol) is prepared a solution of $Na^+C_{10}H_8^-$ in dimethoxyethane, and the solution is cleared by filtration. To this is added at −25 °C over the course of 2 h a solution of **23** (1 g, 1.8 mmol) in 175 mL of dimethoxyethane. The yellow-brown solution, obtained after stirring overnight at room temperature, is brought to dryness *in vacuo*, and naphthalene is removed by sublimation (50 °C, 10^{-4} mbar). The residue is extracted into petroleum ether (40/60), and the solution is reduced to a volume of 4 mL and cooled to −10 °C. Within 1 week the germachromocyclophane **24** is obtained as small black crystals (yield: 90 mg, 4%). ^{1}H NMR (benzene-d_6): δ 4.83 (*o*-H), 4.30−4.38 (*m*-, *p*-H), 0.53 (CH_3). ^{13}C NMR (benzene-d_6): δ 88.2 (ipso-C), 80.9 (d, *o*-C, ^1J(C,H) = 164 Hz), 75.0 (d, *m*-C, 166 Hz), 76.3 (d, *p*-C, 167 Hz), 126.8 (q, CH_3, 126 Hz). MS (EI, 70 eV): *m*/*z* (relative intensity) 412 (M^+, 46.4), 310 ($C_6H_6CrPhGeMe_2^+$, 18.3), 208 ($C_{12}H_{12}Cr^+$, 36.4), 181 ($PhGeMe_2^+$, 14.6), 151 ($PhGe^+$, 7.2), 130 ($C_6H_6Cr^+$, 39.8), 52 (Cr^+, 100). Anal. Calcd for $C_{16}H_{22}CrGe_2$: C, 46.49; H, 5.39. Found: C, 46.82; H, 5.56.

Thermolysis of 18$^\bullet$. About 20 mg of **18$^\bullet$** is gradually heated in an evacuated, sealed tube (5 × 80 mm) at a rate of ∼4 °C min^{-1}. At 135 °C, droplets of a colorless liquid start to condense at cooler sections of the vessel with no apparent change in appearance of solid **18$^\bullet$**. At 160−165 °C, extensive decomposition of **18$^\bullet$** sets in, leaving a black solid as residue. The colorless liquid was subjected to mass spectrometric analysis. MS (EI, 70 eV): *m*/*z* (relative intensity) 258 (Ph_2GeMe_2, 2.2), 243 (Ph_2GeMe, 100), 228 (Ph_2Ge − H, 6), 181 ($PhGeMe_2$, 13), 151 (PhGe, 22). The masses given represent the ^{74}Ge isotopomers.

Acknowledgment. We thank the Deutsche Forschungsgemeinschaft (E.S.: Graduiertenkolleg Metallorganische Chemie) and the Fonds der Chemischen Industrie for financial support of this work.

Supporting Information Available: Tables listing details of crystal data and structure refinement, atomic coordinates and displacement parameters, and bond lengths and angles for **20** (9 pages). Ordering information is given on any current masthead page.

OM970249Y